JOURNAL OF GEOPHYSICAL RESEARCH, VOL. 87, NO. A3, PAGES 1361–1368, MARCH 1, 1982

EUV Emission From Titan's Upper Atmosphere: Voyager 1 Encounter

DARRELL F. STROBEL

Naval Research Laboratory, Washington, D.C. 20375

D. E. SHEMANSKY

Earth and Space Sciences Institute, University of Southern California, Tucson Laboratories, Tucson, Arizona 85711

Analysis of Titan's EUV emission spectra obtained at the Voyager 1 encounter demonstrates that electron impact on N_2 above 3600 km accounts for the bulk of the observed emission short of Lyman α. In conjunction with the UVS solar occultation data it is concluded that N_2 is the major component of Titan's upper atmosphere, with upper limit mixing ratios at 3900 km on NeI, ArI, CO, H_2, and HI of 0.01, 0.06, 0.05, 0.06, and 0.1, respectively. Magnetospheric electrons interact with Titan's sunlit hemisphere to produce a power dissipation rate of $\simeq 2 \times 10^9$ W in the exosphere and $\simeq 3 \times 10^9$ W below the exobase, with optical signatures from numerous N_2 bands, NI, and NII multiplets. The N_2 c_4' (0-0) Rydberg band at 958 Å acts as an optical probe of Titan's exosphere because of transmission losses caused by fluorescence and predissociation. Magnetospheric electron precipitation produces an average dayside electron density of $\simeq 3 \times 10^3$ cm^{-3} between 3600 and 4000 km, the region of bright limb emission. When Titan is within Saturn's magnetosphere, magnetospheric electron impact dissociation of N_2 generates an N atom escape rate of $\simeq 3 \times 10^{26}$ s^{-1} from Titan's exosphere. A nonthermal H atom escape rate of $\simeq 2 \times 10^{26}$ s^{-1} is estimated from magnetospheric electron impact ionization of N_2 followed by reactions with CH_4 and H_2 and recombination to produce hot H atoms.

INTRODUCTION

The presence of N_2 in Titan's atmosphere was first suggested by *Lewis* [1971], on the basis of his accretion model, and by *Hunten* [1972]. The well-known difficulties in ground-based detection of N_2 delayed confirmation of its presence until the Voyager flyby of Titan. Direct evidence for N_2 was obtained from EUV-band emission in the upper atmosphere observed by the ultraviolet spectrometer (UVS) [*Broadfoot et al.*, 1981]. The detection of HCN by the Voyager infrared spectrometer [IRIS, *Hanel et al.*, 1981] and the neutral scale height inferred from the radio occultation experiment [*Tyler et al.*, 1981] also indicate a massive N_2 atmosphere.

In this article we describe observations and analysis of the Voyager 1 EUV emission spectra of Titan, giving results in more detail and giving further analysis of the work first reported by *Broadfoot et al.* [1981]. The observations in the 500-Å–1700-Å region are dominated by the emission spectrum of electron-excited N_2. The spectra contain other emitters, hydrogen in particular, and features that have not been positively identified. We examine the N_2 emission in detail below and discuss the other features briefly. The detailed analysis of the Titan hydrogen component is left to a later publication.

GENERAL CHARACTERISTICS OF THE EUV OBSERVATIONS

The sunlit atmosphere of Titan shows a spectrum characteristic of electron-excited N_2 and a prominent atomic hydrogen Ly-α 1216-Å line. Figure 1 shows a spectrum of the planet dayside emission after subtraction of a synthetic 1216-Å line, representing the average intensity of the sunlit hemisphere. Table 1 gives the intensities obtained from the analysis of this spectrum. Figure 2 shows a scan of emission in the 942-Å–998-Å region, predominantly N_2 bands, and H Ly α emission as a function of altitude above planet center. This limb scan is on the side of the planet facing into the corotating magnetospheric plasma. Emission above 5000 km in Figure 2 is dominated by solar radiation scattering of H Ly α from the interstellar medium and the hydrogen torus [see *Broadfoot et al.*, 1981]. The weak peak at 5000 km, shown in Figure 2 in the nitrogen band region, correlates with strong line emission at 1044 ± 5 Å, as shown in Figure 3. The probable identity is the resonance line of ArI at 1048 Å, but it is difficult to believe that argon is an abundant component of Titan's exosphere. The average spectrum between 4800 km and 4300 km is shown in Figure 4. Many weak features are near the counting noise levels. Real features, in addition to H Ly α in the spectrum of Figure 4, are emission at 657 ± 3 Å and the broad emission in the 900-Å–1100-Å region, which may be weak N_2 bands. The 657-Å feature, identified as being partly composed of NII multiplets at 645 and 671 Å, persists in the observations shown in Figure 2 from 4800 km down to the visible disk with an intensity varying only by a factor of $\simeq 2$, while the N_2-band emission varies by at least an order of magnitude through this same altitude range. Figure 5 shows the averaged spectrum in the 3900-km–3400-km region, which includes the peak emission rate of the N_2 bands at 3660 km. Table 1 gives the estimated intensities for features in this spectrum. Although the emission rates in Table 1 are $\simeq 3$ times brighter in the N_2 bands than in the disk-averaged spectrum of Figure 1, the spectrum is of lower quality because of shorter integration time. The 657-Å feature is not detectable in the earlier disk-averaged spectrum of Figure 1.

The H Ly α emission originates from Titan's atmosphere, the interstellar medium, and the hydrogen torus and exhibits a weak peak at 3900 km in Figure 2, approximately 240 km above the peak in the N_2 Rydberg band emission. On the

This paper not subject to U.S. copyright. Published in 1982 by the American Geophysical Union.

Paper number 1A1209.

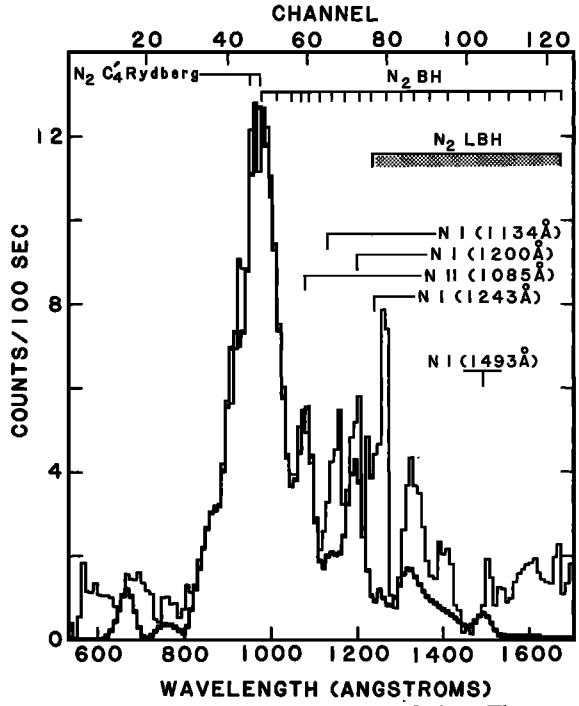

Fig. 1. Averaged dayside disk spectrum of Titan. The accumulated observation time is 7246 s, starting at day 316/21:37 U.T. The spectrum has been reduced by removal of internal instrumental scattering and a 1216 Å synthetic H Ly α line to show the presence of blended features. The heavy overplotted spectrum is a model calculation composed of N_2, NI, and NII emissions excited by electron impact on N_2 (see Table 1). The major nitrogen emissions are indicated on the figure.

dark hemisphere of Titan, the H Ly α line is the only easily detectable emission.

ELECTRON IMPACT ON N_2: DISSOCIATION, IONIZATION, AND RADIATION

The UVS detected the $c_4'\ ^1\Sigma_u^+ - X\ ^1\Sigma_g^+$ 0-0 and 0-1 Rydberg bands of N_2 (N_2 RYD), the NI ($^4S^0$-^4P) multiplet at 1134 Å, and the NII ($^3D^0$-^3P) multiplet at 1085 Å [*Broadfoot et al.*, 1981]. Marginal detection of NI multiplets at 1200 and 1243 Å was also reported. Arguments developed in that paper favor magnetospheric plasma interacting with N_2 in Titan's exosphere as the source of the observed emission from the sunlit hemisphere. Since the threshold for NII (1085-Å) emission from N_2 is 36 eV the exciting particles must have energy in excess of plasma corotation energy. Of the potential candidates the most viable is energetic magnetospheric electrons or accelerated photoelectrons because the protons and heavy ions measured by the Plasma Science Experiment are not sufficiently energetic [*Bridge et al.*, 1981]. Detailed model calculations given below indicate that the N_2 Birge-Hopfield (BH) and Lyman-Birge-Hopfield (LBH) bands as well as other N_2 bands are also present in the spectrum.

The N_2 RYD bands have a small but significant probability of predissociation [*Zipf and McLaughlin*, 1978]. The branching ratio of the 0-0 band to the 0-1 band is 1:0.17 [*Zipf et al.*, 1982]. Thus the observation of the 0-0 band at 958 Å places an upper limit on the permissible optical depth between the excitation source and the Voyager spacecraft. On the basis of its oscillator strength and laboratory data (E. C. Zipf, private communication, 1980) the N_2 RYD band emission in the disk-averaged spectrum of Figure 1 must originate in the upper 10^{15} cm^{-2} of N_2 in Titan's atmosphere, i.e., essentially the exosphere, although it is not clear whether all of the emission originates at the same altitude. The oscillator strength of 0.22 [*Zipf and McLaughlin*, 1978] gives an average cross section over the 0-0 band of $\simeq 10^{-15}$ cm^2. Individual rotational lines have cross sections at line center that exceed 10^{-12} cm^2. The relative intensities of the N_2 RYD 0-0, 0-1, and 0-2 bands given in Table 1 are indicative of optical thickness in both the 0-0 and 0-1 bands, which suggests a nonthermal population of N_2 vibrational levels in the exosphere. These constraints eliminate solar photons and photoelectrons as primary excitation sources for the observed emission in the N_2 Rydberg bands, although other N_2 emissions may originate at lower altitudes.

Because the NI (1134-Å) multiplet does not have comparable intensity to NI (1200 Å) and is much weaker in intensity than NII (1085 Å), the dominant excitation source must be electron impact on N_2 rather than N(^{4}S) or N(^{2}D). From the relevant cross section data of *Winters* [1966], *Aarts and DeHeer* [1971], *Mumma and Zipf* [1971], *Stone and Zipf* [1973], *Zipf and McLaughlin* [1978], *Zipf et al.* [1982], and *Zipf and Gorman* [1980], some cross sections for electron impact processes on N_2 are given in Table 2. From these cross sections the intensity ratio N_2 RYD/N_2 BH should be $\simeq$4 for an electron energy distribution of $T_e = 2 \times 10^5$ K (Table 1), but the observations indicate N_2 RYD/N_2 BH = 1 and 0.5 on the disk average and bright limb spectra (Figures 1 and 5), strongly indicative of N_2 BH band emission below the exobase where the N_2 RYD bands are optically thick. The modeled ratio N_2 RYD/NII 1085 = 8.6, as compared to the observed values of 2.3 and 1.1, indicates a similar optical depth effect. At a different temperature electron energy distribution the estimated optical depths would not be the same. With the exception of features that are optically thick the inferred intensities given in Table 1 are in reasonable agreement with excitation cross sections obtained by *Zipf and McLaughlin* [1978].

The observations are analyzed by the application of synthetic spectra of the known emitters. Figures 1 and 5 show model calculations in comparison with the disk average and bright limb spectra. The calculations are based on the known products of electron-excited N_2, using experimental cross sections when available. The various separable emission products were synthesized and fitted to the observed spectra to obtain system intensities. A comparison of the reduced intensities was then made with model calculations for different electron energy distributions. The calculations shown in Table 1 apply Maxwell-Boltzmann electron energy distributions under optically thin conditions. The high-temperature (10^6 K) distribution is representative of primary electron excitation in the exosphere. The low-temperature (2×10^5 K) distribution is roughly equivalent to the dominant (secondary) electron distribution produced in an atmosphere at the exobase and lower altitudes, where the differential flux of secondary electrons take on an E^{-n}, $n \simeq 1.4$ energy dependence [cf. *Shemansky et al.*, 1972]. It is clear that excitation processes are simplified in the model since several features in the observations are not modeled at all, and the disk average/bright limb spectra show distinct real differences. The model calculations shown in the figures include

TABLE 1. Titan Data

Species	Observed Intensity, R*		Predicted Intensity	
	Disk Average	Bright Limb	$T_e = 10^6$ K	$T_e = 2.0 \times 10^5$ K†
N_2 RYD (0, 0) 958.0	12	21	212	110
N_2 RYD (0, 1) 981.0	8.6	21	36	18.7
N_2 RYD (0, 2) 1003.2	7.0	5.8	4.2	2.2
N_2 RYD (3, 0) 903.6	5.6	1.8		
N_2 RYD (3, 2) 944.5	0.2	2.0		
N_2 RYD (3, 3) 964.0	0.5	4.1		
N_2 RYD (4, 0) 886.8	6.3	1.0		
N_2 BH (1, v″)	25	97	33	33
N_2 BH (5, 0) (954.0 Å)	0.3	2.7		
N_2 LBH system	96	290	180	426
N_2 b′ VAL (3, 0) (942.5 Å)	0.3	2.9		
N_2 b′ VAL (17, 0) (866.9 Å)	8.2	1.4		
N_2 b′ VAL (9, 0) (907.5 Å)	2.2	0.7		
N_2 $m = 5$ $^1\Pi$ $v = 0$ (835.4 Å)	1.7	1.4		
N_2 c_3 $^1\Pi_u$ (2, 0) (920.0 Å)	6.0	5.0		
NI (1493 Å)	15	49	61	21
NI (1412 Å)	0.8	2.6	4	1.1
NI (1327 Å)	1.0	3.2	2.7	1.5
NI (1311 Å)	3.1	11	9.6	4.9
NI (1243 Å)	8.0	27	39	11.6
NI (1200 Å)	30	102	166	43
NI (1177 Å)	5.3	18	15	8.2
NI (1168 Å)	5.3	18	15	8.4
NI (1164 Å)	1.1	3.6	3.4	1.6
NI (1134 Å)	7.9	27	24	12
NII (1085 Å)	12	42	88	15
NII (916 Å)	1.0	3.5	11.5	1.2
NII (776 Å)	0.3	1.1	2.3	0.4
NII (747 Å)	0.3	1.1	2.6	0.4
NII (671 Å)	0.8	2.8	6.3	1.0
NI + $e \rightarrow$ NII + 2e (645 Å)	<0.2	<2.0		
H_2 (Lyman & Werner)	<16			
HI (1216 Å)	700	700		
CO 4th pos. (3, 0 (1447 Å)	<2			
NeI (736 Å)	<0.2			
ArI (1048 Å)	<6			
$[N_eI]/[N_2]$	1×10^{-2}		$R = 3900$ km	
[ArI]/[N_2]‡	6×10^{-2}		[$N_2 = 2 \times 10^8$ cm^3	
$[H_2]/[N_2]$	6×10^{-2}			
[CO]/[N_2]	5×10^{-2}			
[HI]/[N_2]	1×10^{-1}			

*See Figures 1 and 5.

†Based on $e + N_2$ in optically thin gas for 2×10^{10} W average input to the dayside planet. An electron temperature of 2×10^5 K is approximately equivalent to an auroral secondary electron differential flux distribution of the form E^{-n} with $n = 1.4$. An electron temperature of 10^6 K may be taken as appropriate for primary electron excitation above the exobase. For $T_e = 2 \times 10^5$ K, the inferred input is 5×10^9 W.

‡With the *Smith et al.* [1982] eddy diffusion profile, the ratios for NeI and ArI are 0.002 and 0.6, respectively, at the surface.

the significant lines of NI; the N_2 LBH, BH, and RYD systems; the N_2 Rydberg $^1\Pi_u$ c_3 (2-0) and c_4 (0,0) bands; the N_2 Rydberg $^1\Sigma_u^+$ c_4' ($v' = 3, 4$) band systems; the N_2 valence b' $^1\Sigma_u^+$ (17,0), (9,0), and (3,0) bands; and the NII multiplets at 645, 671, 747, 776, 916, and 1085 Å (see Tables 1 and 2). The 900-Å to 1200-Å region of the bright limb spectrum (Figure 5) shows fewer significant emission features than the disk average spectrum (Figure 1) and fits the model calculations more satisfactorily. The model fit to both spectra depends rather critically on the strong presence of the N_2 BH bands, which appear in the 980-Å–1250-Å region. The model calculations give a best fit to the observations with a $T_e \simeq 2 \times 10^5$ K electron energy distribution, which is characteristic of auroral secondary electrons. These electrons would be expected to generate most of the excitation from magnetospheric electron precipitation, rather than the primary electrons. The intensity ratio of N_2 BH/N_2 LBH/NII 1085 Å is sensitive to electron energy distribution as illustrated in Table 1. The difficulty in reconciling the observations with the model calculations is that the deduced intensities of the NII 1085-Å, N_2 BH, and N_2 LBH emissions cannot be produced with a single electron energy distribution. The observed N_2 BH/NII 1085-Å ratio requires a dominance of low-energy electrons, whereas the N_2 BH/N_2 LBH ratio requires a dominance of high-energy electrons. It is possible that the observations contain a mix of low- and high-altitude emissions with different characteristic electron temperatures for excitation, since the bright limb spectrum (Figure 5)

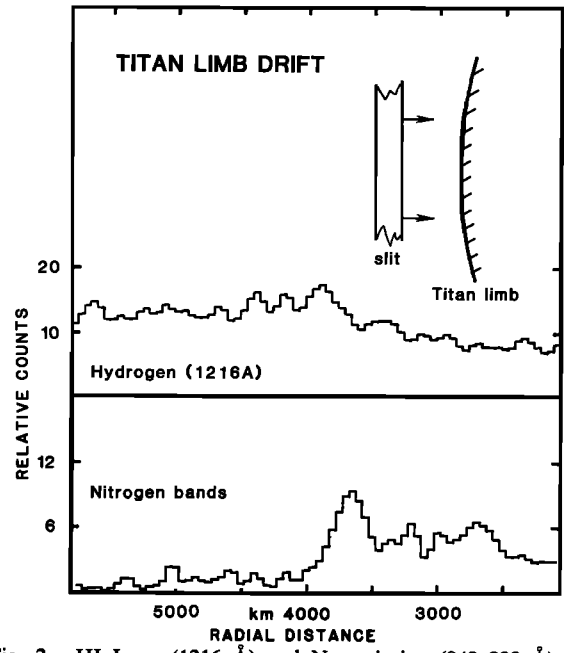

Fig. 2. HI Ly a (1216 Å) and N_2 emission (942–998 Å) as a function of altitude above planet center. The emission structure is described in the text. The slit width, drawn to scale on the figure, is about 200 km; slit length 1700 km. The observational sequence is UTBLM2 starting at about day 317/3:00 U.T.

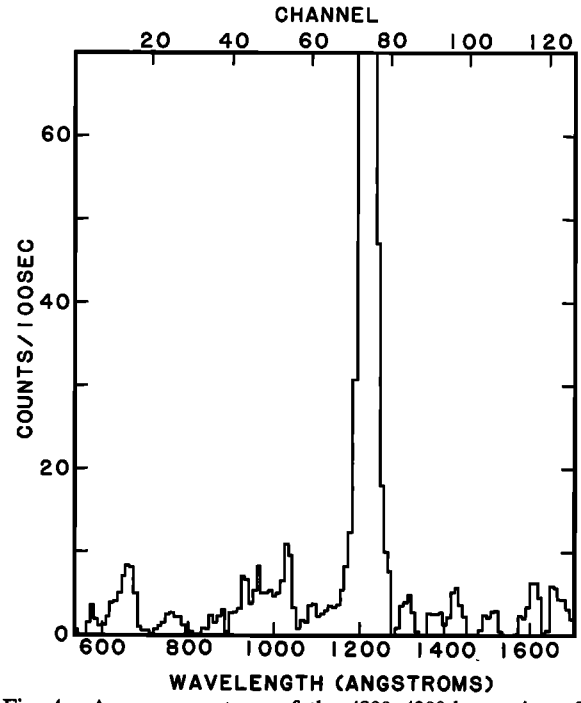

Fig. 4. Average spectrum of the 4800–4300-km region of the plot in Figure 2. A distinct feature at 657 ± Å is observed along with possible weak N_2 band emission.

shows an apparent N_2 RYD (0,1)/(0,0) band ratio indicating an optically thin source (ratio <1), whereas the N_2 RYD/N_2 BH ratio is characteristic of an optically thick source. To this extent, estimates of emission altitude are uncertain, and some of the emission may arise below the exobase region. We reiterate that the 850–1200-Å region of the spectrum is complex and that optically thick N_2 bands whose excited states predissociate and branch to longer wavelengths are exceedingly difficult to accurately model. Some additional features in this region that are shown by the disk average spectrum (Figure 1) are NI and NII transitions produced by electron impact on N_2. *Fischer et al.* [1980] and *Morgan and*

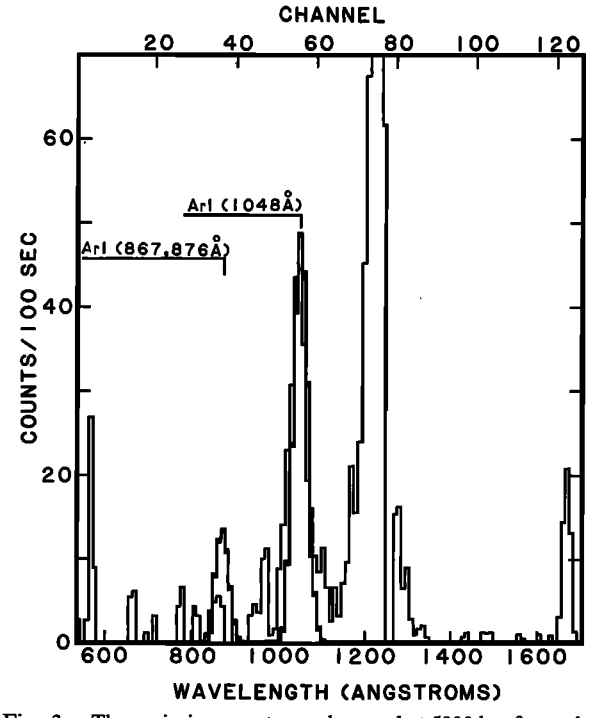

Fig. 3. The emission spectrum observed at 5000 km from planet center. The spectral feature at 1044 ± 5 Å is not detected at other altitudes. The heavy plotted spectrum is a model calculation of ArI excited by electrons at a temperature of 10^5 K.

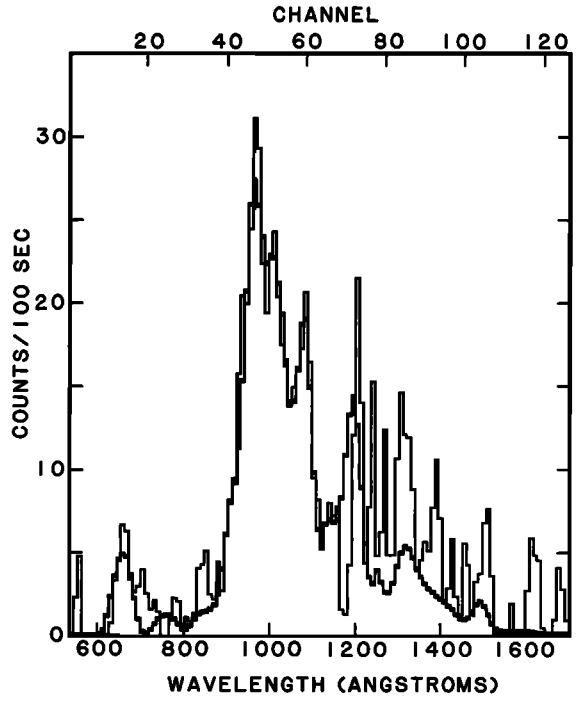

Fig. 5. Bright limb spectrum of Titan in the 3900–3400-km region containing the N_2 emission peak at 3660 km (see Figure 2). Integration time 290 s. The heavy overplotted spectrum is a model calculation as described in Figure 1. Table 1 lists the estimated intensities of the modeled spectrum.

TABLE 2. Electron Impact Cross Sections for N_2

E (eV), cm^2	30	50	80–120
(N_2^+)	1.1 (−16)	1.5 (−16)	1.9 (−16)
(N^+)	5 (−18)	2.8 (−17)	6.0 (−17)
(N(^{2}D) + N(^{4}S))	1.4 (−16)	1.6 (−16)	1.7 (−16)
(N_2, 958 + 981 Å)	6.5 (−18)	1.0 (−17)	1.1 (−17)
(NII, 1085 Å)	0	1.4 (−18)	3.9 (−18)
(NII, 916.0 Å)	0	9.4 (−20)	3.8 (−19)
(NI, 1492.6 Å)	6.4 (−19)	1.9 (−18)	2.7 (−18)
(NI, 1310.97 Å)	2.5 (−19)	4.6 (−19)	4.5 (−19)
(NI, 1200 Å)	1.2 (−18)	3.7 (−18)	6.7 (−18)
(NI, 1176.9 Å)	2.8 (−19)	6.5 (−19)	5.9 (−19)
(NI, 1164.3 Å)	6.8 (−20)	1.6 (−19)	1.6 (−19)
(NI, 1134 Å)	5.6 (−19)	1.0 (−18)	1.2 (−18)
N_2 BH $v' = 1$	2.0 (−18)	2.0 (−18)	1.4 (−18)
N_2 LBH	2.4 (−17)	1.3 (−17)	6.4 (−18)

Mentall [1981] show N_2 laboratory discharge spectra containing N_2-band emission at 867 Å and 887 Å and NII lines at 645, 671, 747, 776, and 916 Å that account for some of the features in the disk-averaged spectrum of Figure 1. On the other hand the unidentified emissions longward of 1250 Å at the 1330-, 1400-, and 1600-Å regions are not attributable to N_2 or N_2 dissociation products.

Using the model calculation shown in Table 1, we require a disk average (hemisphere) energy deposition rate of ≈0.05 ergs cm^{-2}s^{-1} and a total of 5×10^9 W on the basis of LBH emission. This sets a lower limit on energy deposition rate since the modeled N_2 LBH bands are a lower limit in the synthesis of the observed emission. These rates produce 9×10^8 cm^{-2}s^{-1} N_2^+ ions, 1.8×10^9 NI atoms, and 1.6×10^8 cm^{-2}s^{-1} NII ions. The approximate source altitude of the majority emission is estimated to be ≈3800 ± 200 km (where $[N_2] = 5 \times 10^8$ cm^{-3}, *Smith et al.*, this issue). This is not necessarily in conflict with the bright limb peak observation at 3660 km since the emission is not symmetrical and the bright limb observation probably represents a lower limit to the emission altitude, especially for optically thick lines. The emission is observed only from the sunlit hemisphere (away from Saturn) and preferentially in the quadrant facing into the corotating magnetospheric plasma.

UPPER LIMIT ON CO ON TITAN

Upper limits on CO in Titan's upper atmosphere can be obtained from the absence of distinct features in the Voyager UVS spectrum because of CO $A^1\,\Pi - X^1\,\Sigma$ (3-0) band emission at 1447 Å. The absence of any feature at 1447 Å gives an upper limit intensity of 2 R for the 3-0 4th positive band of CO, which when coupled with the e + CO cross section from *Mumma et al.* [1971] and compared with the N_2 BH bands, produces an upper limit of $[CO]/[N_2] = 0.05$ in the upper atmosphere. With identical masses this upper limit should apply to the lower atmosphere as well.

Hydrogen

Electron excitation of H_2 produces strong emission in the EUV Lyman and Werner bands. The structure of these band systems have been modeled (D. E. Shemansky et al., unpublished manuscript, 1982), and a limit on their contribution to the emission spectrum was estimated by *Broadfoot et al.* [1981]. The N_2 model calculations applied to the observations in the present work have reduced the estimated H_2 emission upper limit by a factor of ≈3 to $[H_2]/[N_2] < 0.06$ as given in Table 1. Electron excitation of HI produces Lyman series radiation measurable to the Rydberg limit. Model calculations (D. E. Shemansky et al., unpublished manuscript, 1982), of the relative count rate in the EUV instrument at channel 41 (910 Å), where optical depth effects are minimized for HI emission, indicate an upper limit of 150 R in 1216-Å radiation for electron excitation. This places an upper limit of $[HI]/[N_2] < 0.1$ at ≈3800 km. The upper limits for both $[H_2]$ and [HI] are comparable to the measured CH_4 density [Smith *et al.*, this issue]. *Samuelson et al.* [1981] have determined an H_2 mixing ratio of 0.002 in the lower atmosphere from Voyager IRIS data.

Argon and Neon

Upper limits on argon and neon estimated by *Broadfoot et al.* [1981] are retained as satisfactory estimates in the present work on the dayside disk and bright limb spectra. The spectrum for a sharply peaked region at 5000 km in the limb scan displayed in Figure 3 exhibits a strong line at 1044 ± 5 Å close to the location of the ArI 1048-Å resonance line. The intensity of the observed line is 90 R and would require what appears to be an unreasonable amount of ArI at that altitude. The projected density $[N_2] = 1.3 \times 10^4$ cm^{-3} from the EUV occultation experiment [Smith *et al.*, this issue] would require an electron density $[e] = 1 \times 10^3$ cm^{-3} at a temperature of $T_e = 1 \times 10^6$ K to account for the weak feature at 960 Å (N_2 RYD) in Figure 3. If the feature at 1044 Å is then attributed to ArI, we require [ArI] = 10^4 cm^{-3}, giving $[ArI]/[N_2] \simeq 1$ at 5000 km and implying that argon is the major constituent of the lower atmosphere. Note that the 1048-Å line is not detected at higher or lower altitudes (see Figures 3, 4, 5). However, the nature of the data indicates that this line is real and extends over an altitude range of ≈250 km centered at 5000 km. Figure 3 shows a model calculation of ArI emission for an electron temperature of $T_e = 10^5$ K and points out an added difficulty. The absence of a strong ArI feature at 866–876Å requires a much lower electron temperature than 10^5 K for collisional excitation by electrons. Another possible excitation mechanism is ArII + $N_2 \rightarrow N_2^+$ + ArI, but again we require highly unusual physical circumstances.

Other Emission Features

The persistent feature at 657 ± 3 Å that appears in the averaged spectrum in the 4800–4300-km range (Figure 4), in the region of the peak N_2-band emission at 3660 km and in spectra just inside the planet's limb as part of the bright limb scan, does not show a correlation with the N_2 bands. This is consistent with our identification of this feature as partly belonging to NII emission from electron impact on NI. However, our analysis requires an additional emission line at ≈657 Å to adequately account for this feature (see Figure 5). This emission is clearly associated with the planet because the feature is not measurable in spectra above 5000 km. The intensity of the feature shows little or no Chapman effect since in the 4800–4300-km region it is ≈5 R; at 3660 km, ≈10 R; and ≈1 R in the disk-averaged spectrum. However, absorption of the radiation by N_2 may be important and would significantly modify the limb profile. A search for plausible source specie has produced no result for the additional emission line.

The spectrum of Figure 1 contains several emissions that may not be attributable to N_2, NI(^{4}S), or NII. There are

TABLE 3. Ion Chemistry

Reaction			Yield
$e^* + N_2$	→	$N_2^+ + 2e$	0.45
	→	$N^+ + N + 2e$	0.10
	→	$N(^2D) + N(^4S)$	0.45
$N_2^+ + CH_4$	→	$CH_3^+ + N_2 + H + 1.3$ eV	0.92
	→	$CH_2^+ + N_2 + H_2 + 0.7$ eV	0.08
$N^+ + CH_4$	→	$CH_3^+ + N + H + 0.3$ eV	0.53
	→	$CH_4^+ + N + 1.8$ eV	0.04
	→	$H_2CN^+ + H + H + 3.3$ eV	0.32
	→	$HCN^+ + H_2 + H + 1.35$ eV	0.10
$HCN^+ + CH_4$	→	$H_2CN^+ + CH_3 + 2.9$ eV	0.84
	→	$C_2H_3^+ + NH_2 + 0.8$ eV	0.16
$H_2CN^+ + e$	→	$HCN + H$	
$N_2^+ + H_2$	→	$H_2H^+ + H$	
$N_2H^+ + e$	→	$N_2 + H$	
$N^+ + H_2$	→	$NH^+ + H$	
$NH^+ + N_2$	→	$N_2H^+ + N$	

features at 1160 Å, ≈1250 Å, 1330 Å, 1400 Å, ≈1510 Å, and in the 1550–1670-Å region. Possible contributors to these emissions are CI, NI(^{2}D), and CII. The ion CII produces strong features at 904 Å, 1037 Å and 1335 Å from the process e + CII. The distributions of CII emission produced by e + CI and $e + CH_4$ have not been investigated. Emission from CI ground-state connected lines appear at 945 Å, 1158 Å, 1189 Å, 1193 Å, 1261 Å, 1277 Å, 1280 Å, 1329 Å, 1561 Å, and 1657 Å, suggesting a possibility of CI contributions to the observed spectrum, although the emission spectrum has not been modeled. Electron impact on NI (^{2}D), which may have appreciable concentration in the upper atmosphere, could produce anomalous intensities of the doublet multiplets at 1164, 1168, 1177, 1243, 1311, 1320, 1327, 1412, and 1493 Å. Based on the source strength of N(^{2}D) in the exosphere given below we estimate an N(^{2}D) density at the exobase of $\sim 2 \times 10^6$ cm^{-3} and exosphere column density of 4×10^{13} cm^{-2} with loss processes of radiative decay, quenching by CH_4, and molecular diffusion. Assuming electron impact on N(^{2}D) has a comparable cross section to e + N(^{4}S) for electronic excitation, we estimate that ~100 R of the above doublet multiplet radiation would be produced on the basis of the observed N_2 RYD band emission from Titan's exosphere. For some of these multiplets the atmosphere will be moderately optically thick at line center, even in the exosphere.

Part of the emission spectrum at 1400 Å and the 1550–1670-Å region may be due to solar radiation albedo. If all of the emission were attributed to solar radiation scattering, we would require a geometric albedo in the range 0.1–0.15. These are rather large albedos in comparison with the value 0.025, which was obtained by *Caldwell et al.* [1981] at 2200 Å. Flourescence of C_2H_2 emerges in the visible wavelengths [*Okabe*, 1975] and also could not account for the observed features.

N_2 PHYSICAL CHEMISTRY

At the exobase, only 0.33 eV is needed for N atoms to escape Titan. For N_2 dissociation via singlet states it is possible to estimate the fraction of N atoms produced at energies in excess of 0.33 eV with the dipole allowed oscillator strengths of *Wight et al.* [1976]. No estimate for excitation of triplet N_2 states by low-energy electrons can be made, however. Triplet states constitute a minor fraction of the electron impact cross section for dissociation. Since the oscillator strengths, cross sections, and transition probabilities are all proportional to each other, the integrated oscillator strength over the 12.1–19.0-eV region, when weighted by the dissociation probability, must be proportional to the integrated electron impact dissociation cross section for N_2. Because predissociation of N_2 singlet states leads to N(^{4}S) + N(^{2}D) products [cf. *Oran et al.*, 1975], only N_2 singlet states excited to 9.76 + 2.38 + 2(0.33) = 12.8 eV and above will produce escaping N atoms. The approximate fraction of N atoms originating from states in the 12.8–19-eV region is 0.85. Thus on Titan, ≈85% of the dissociated N atoms have sufficient energy to escape, considerably larger than the 16% calculated for Mars [cf. *McElroy et al.*, 1976]. With the usual assumption that half are directed into the upward hemisphere the conclusion is that ≈40% of the N atoms produced in the exosphere escape. From the disk-averaged intensities for the N_2 RYD bands given in Table 1, which must originate from the exosphere, we infer a magnetospheric dissipation rate in the exosphere alone of ≈0.02 ergs cm^{-2} s^{-1}, approximately 0.4 of the total dissipation rate in the atmosphere. Thus 7×10^8 N atoms are produced in the exosphere, approximately $2\pi R_{ex}^2 \times 7 \times 10^8 \times 0.4 \simeq 3 \times 10^{26}$ N atoms s^{-1} are supplied to the magnetosphere and/or solar wind from Titan. This is equivalent to the loss of 0.2 of the present N_2 atmosphere over the age of the solar system. However we note that an estimate of long-term loss is subject to the considerable uncertainty in temporal morphology of the position of the solar bow shock region. The net production rate of N atoms below the exobase is $\simeq 1 \times 10^9$ cm^{-2} s^{-1}, of which one half are in the metastable ^{2}D level [cf. *Oran et al.*, 1975]. A global average (× 0.5) and an adjustment of the production rate/flux in Titan's spherical atmosphere to the surface, R_T, by $(R_{ex}/R_T)^2$ yields a net production rate of 8×10^8 cm^{-2} s^{-1} for each N(^{4}S) and N(^{2}D) by magnetospheric interaction.

As indicated in a previous section, magnetospheric interaction with Titan's upper atmosphere leads to the production of substantial N_2^+ and N^+, $\simeq 9 \times 10^8$, and 1.8×10^8 cm^{-2} s^{-1}, respectively. In Table 3 the probable ion chemistry of nitrogen ions is briefly sketched; all ion molecule reactions are of order 10^{-9} cm^3 s^{-1} with one exception, $NH_3^+ + H_2$ [*Huntress et al.*, 1980]; N_2^+ is rapidly converted to CH_3^+ and CH_2^+ with the N_2 bond unbroken. NII reacts rapidly with CH_4 to form NI atoms and hydrocarbon ions with ≈57% yield and H_2CN^+ and HCN^+ with 32% and 10% yield, respectivey. HCN^+ is rapidly converted to H_2CN^+ with $C_2H_3^+$ a minor path. Further reaction of H_2CN^+ is not possible with hydrocarbons [*McEwan et al.*, 1981], and it is most probable that this terminal ion dissociatively recombines to HCN. Thus approximately 40% of all NII would be converted directly to HCN, with the remaining 60% converted to NI atoms. However, the density structure of Titan's exosphere is still uncertain (see below) and H_2 may be as abundant as CH_4, even though it has an N_2 scale height as a consequence of rapid escape. (*Smith et al.* this issue, give a CH_4 mixing ratio of 0.08 at 3700 km, whereas *Samuelson et al.* [1981] obtained an H_2 mixing ratio of 0.002 in the lower atmosphere.) If $[H_2] \gg [CH_4]$, then NII would be converted to N and N_2^+ to N_2 as shown in Table 3. In either case the rapid recombination of terminal hydrocarbon and H_2CN^+

ions would indicate a quick decay of the ionosphere at sunset and a negligible nighttime ionosphere. If we assume that ionization by magnetospheric interaction is produced over the altitude range 3600–4100 km with a recombination rate of 3×10^{-6} cm^3 s^{-1}, appropriate for hydrocarbon ions, then an average dayside electron density of $\simeq 3 \times 10^3$ cm^{-3} would be maintained.

Note that all reactions are considerably exothermic, and the light fragment, mostly H atoms, may be released with velocity in excess of the escape velocity. In the case of dissociative recombination the H atoms will be translationally hot. On the basis of N_2^+ and NII production rates in the exosphere and the assumption of one hot H atom per ionization, the nonthermal escape rate is $\simeq 2 \times 10^8$ H atoms cm^{-2} s^{-1} in the upward hemisphere on the dayside for a total of 2×10^{26} s^{-1} supplied to Saturn's magnetosphere. Since these H atoms have considerable velocity they may populate the 'torus' observed by the Voyager UVS at Lyman α, extending from Titan inward to Rhea [*Broadfoot et al.*, 1981].

In addition, solar radiation produces photoelectrons in Titan's thermosphere that ionize and dissociate N_2 and excite UV radiation from N_2 RYD bands. The radiation from this source will be trapped at these large optical depths ($\simeq 100$) and converted to chemical energy. Radiation produced by the N_2 LBH and BH bands excited by photoelectrons may be observed by the UVS. The bulk of the photoelectrons of interest will have energies of 25–35 eV and hence cannot efficiently produce NII (1085-Å) radiation, which has a threshold of 36 eV. Based on the solar spectrum, approximately 2.5×10^8 photoelectrons cm^{-2} s^{-1} will be produced between 25–35 eV and $\simeq 10^8$ cm^{-2} s^{-1} with energies 40–55 eV. The latter photoelectrons will produce less than 1 R of NII (1085 Å). If one ion pair is produced per photoelectron, then with the cross section data in Table 1 a production rate of $\simeq 4 \times 10^8$ cm^{-2} s^{-1} for each N(^{2}D) and N(^{4}S) atoms and $\simeq 4 \times 10^7$ NII cm^{-2} s^{-1} will result. Dissociative ionization of N_2 by solar photons will produce $\simeq 10^8$ NII cm^{-2} s^{-1}. Photodissociation of N_2 by predissociation in the numerous bands between 800–1000 Å leads to a production rate of $\simeq 10^8$ cm^{-2} s^{-1} for each N(^{2}D) and N(^{4}S) [*Oran et al.*, 1975]. With a global average and adjustment to Titan's surface, solar photons and photoelectrons generate N(^{2}D), N(^{4}S), and NII at a rate of $\simeq 2.5 \times 10^8$, 2.5×10^8, and 7×10^7 cm^{-2} s^{-1}, respectively. These rates are less than production rates by magnetospheric electrons.

Cosmic rays produce approximately 10^8 ion pairs cm^{-2} s^{-1} in Titan's lower stratosphere [*Capone et al.*, 1980], of which 20% are NII. In addition, approximately 7×10^7 cm^{-2} s^{-1} of each N(^{2}D) and N(^{4}S) will result from secondary electrons dissociating N_2. Higher hydrocarbons can be produced via subsequent ion chemistry [*Capone et al.*, 1980].

DISCUSSION

The major difference between the preliminary analysis [*Broadfoot et al.* 1981] of the Voyager 1 EUV observations of Titan and the present work is the conclusion that some strong emission in the 900–1500-Å region originates deep in the atmosphere, where the N_2 RYD bands are optically thick. This difference arises simply from the fact that the necessary detailed model calculations were not available at the time of the *Broadfoot et al.* [1981] 30-day report. The best support for this conclusion from the data is the N_2 RYD/N_2 LBH intensity ratio, which is an order of magnitude lower than an optically thin model calculation.

The conclusion that the N_2 RYD bands are optically thick in the region of strong N_2 LBH emission requires an increase in estimated rate of electron energy deposition, 5×10^9 W (0.05 ergs cm^{-2} s^{-1}), over the *Broadfoot et al.* [1981] estimate of 0.02 ergs cm^{-2} s^{-1}, which applies only to the exosphere. The new energy deposition requirements exceed the solar EUV deposition rate by a factor of $\simeq 10$ and emphasize the point made in the earlier work that photoelectrons cannot directly provide the required energy. However it is possible that photoelectrons serve as a catalyst for the generation of energetic electrons, since we do not observe N_2 emission from the darkside atmosphere. The altitude at which most of the energy is deposited is almost certainly above 3600 km ($[N_2] = 6 \times 10^9$cm^{-3}), where the vertical N_2 abundance is $\simeq 4 \times 10^{16}$ cm^{-2}, the point at which production of photoelectrons is near its peak (see note added in proof). We arrive at this conclusion because the bright limb observations, which peak at 3660 km in N_2 emission, have no significant CH_4 absorption effects. Here the slant path CH_4 optical depth at 960 Å is $\simeq 1$. The bright limb emission peak at 3660 km must then be taken as a minimum altitude of maximum energy deposition. It is possible that the region of maximum emission in the N_2 BH bands is as low as 3800 km ($[N_2] = 5 \times 10^8$ cm^{-3}), where the vertical optical depth to the N_2 RYD (0, 0) band is $\gg 1$.

The Titan airglow observations certainly require further analysis with more comprehensive model calculations in order to understand the complexity of the excitation processes. There are a number of unidentified emissions that apparently do not originate with N_2 or its dissociation products. The phenomenon at 5000 km is difficult to explain with plausible physical processes. The unidentified feature at 657 ± 3 Å must be produced at very high altitude since it is observed in the 4800–4300-km region and does not show a strong dependence on N_2 column depth in lower regions of the bright limb scan.

Note added in proof: The structure of the N_2 LBH system under optically thick conditions shows the development of spectral shapes similar to those in the observed data between 1300 Å and 1450 Å. A rough estimate indicates that an optically thick LBH model could produce an approximate factor of 4 increased emission rate at the source. The difficulty discussed in the text relating to the N_2 BH/N_2 LBH/NII 1085-Å emission ratio would then tend to be removed. However, this alternate explanation of excitation conditions would require a factor of 4 increase in energy deposition. Moreover, the majority of the deposited energy must then occur at much greater depths in the atmosphere. The energy deposition rate given in the text should thus be regarded as the minimum rate that can be tolerated in the interpretation of the data. A more definitive conclusion in regard to the excitation characteristics will require further, more refined, model calculations.

Acknowledgments. The authors wish to thank E. C. Zipf for providing valuable discussion and laboratory data analysis prior to publication, G. R. Smith for valuable discussion, and T. Forrester for his work on data acquisition and reduction.

This work is supported under NASA contracts NAS7-100 and

NAGW-106 of the Planetary Sciences Division and the Office of Planetary Atmospheres.

The Editor thanks Y. L. Yung and R. W. Carlson for their assistance in evaluating this paper.

REFERENCES

Aarts, J. F. M., and F. J. DeHeer, Emission cross sections for NI and NII multiplets and some molecular bands for electron impact on N_2, *Physica, 52,* 45–73, 1971.

Bridge, H. S., et al., Plasma observations near Saturn: Initial results from Voyager 1, *Science, 212,* 217, 1981.

Broadfoot, A. L., et al., Extreme ultraviolet observations from Voyager 1 encounter with Saturn, *Science, 212,* 206, 1981.

Caldwell, J., T. Owen, A. R. Rivolo, V. Moore, G. E. Hunt, P. S. Butterworth, Observations of Uranus, Neptune and Titan by the International Ultraviolet Explorer, *Astron. J., 86,* 298, 1981.

Capone, L. A., J. Dubach, R. C. Whitten, S. S. Prasad, and K. Santhanam, Cosmic ray synthesis of organic molecules in Titan's atmopshere, *Icarus, 44,* 72, 1980.

Fischer, F., G. Stasek, and G. Schmidtke, Identification of auroral EUV emissions, *Geophys. Res. Lett., 7,* 1003, 1980.

Hanel, R., et al., Infrared observations of the Saturnian system from Voyager 1, *Science, 212,* 192, 1981.

Hunten, D. M., The atmosphere of Titan, *Comments Astrophys. Space Phys., 4,* 149, 1972.

Huntress, W. T., M. J. McEwan, Z. Karpas, and V. G. Anicich, Laboratory studies of some of the major ion-molecule reactions occurring in cometary comae, *Astrophys. J. Suppl. Ser., 44,* 481, 1980.

Lewis, J. S., Satellites of the outer planets: Their physical and chemical nature, *Icarus, 15,* 174, 1971.

McElroy, M. B., T. Y. Kong, Y. L. Yung, and A. O. Nier, Composition and structure of the Martian upper atmosphere: Analysis of results from Viking, *Science, 194,* 1295, 1976.

McEwan, M. J., V. G. Anicich, and W. T. Huntress, Jr., An ICR investigation of ion-molecule reactions of HCN, *Int. J. Mass Spectrom. Ion Phys., 37,* 273, 1981.

Morgan, H. D., and J. Mentall, EUV studies of N_2 and O_2 produced by low-energy electron impact, *Eos Trans. AGU, 62,* 338, 1981.

Mumma, M. J., and E. C. Zipf, Dissociative excitation of vacuum-ultraviolet emission features by electron impact on molecular gases, 2, N_2, *J. Chem. Phys., 55,* 5582, 1971.

Mumma, M. J., E. J. Stone, and E. C. Zipf, Excitation of the CO Fourth Positive band system by electron impact on carbon monoxide and carbon dioxide, *J. Chem. Phys., 54,* 2627, 1971.

Okabe, H., Photodissociation of acetylene and bromoacetylene in the vacuum ultraviolet: Production of electronically excited C_2H and C_2, *J. Chem. Phys., 62,* 2782, 1975.

Oran, E. S., P.S. Julienne, and D. F. Strobel, The aeronomy of odd nitrogen in the thermosphere, *J. Geophys. Res., 80,* 3068, 1975.

Samuelson, R., R. Hanel, V. Kunde, and W. C. Maguire, The mean molecular weight and hydrogen abundance of Titan's atmosphere, *Nature, 292,* 688, 1981.

Shemansky, D. E., T. M. Donahue, and E. C. Zipf, N_2 positive and N_2^+ band systems and the energy spectra of auroral electrons, *Planet. Space Sci., 20,* 905, 1972.

Smith, G. R., D. F. Strobel, A. L. Broadfoot, B. R. Sandel, D. E. Shemansky, and J. B. Holberg, Titan solar occultation in the EUV from Voyager 1, this issue, 1982.

Stone, E. J., and E. C. Zipf, Excitation of atomic nitrogen by electron impact, *J. Chem. Phys., 58,* 4278, 1973.

Tyler, G. L., V. R. Eshleman, J. D. Anderson, G. S. Levy, G. F. Lindal, G. E. Wood, and T. A. Croft, Radio science investigations of the Saturn system with Voyager 1: Preliminary results, *Science, 212,* 201, 1981.

Wight, G. R., M. J. Vander Wiel, and C. E. Brion, Dipole excitation, ionization, and fragmentation of N_2 and CO in the 10–60 eV region, *J. Phys. B: Atom. Molec. Phys., 9,* 675, 1976.

Winters, H. F., Ionic absorption and dissociation cross section for nitrogen, *J. Chem. Phys., 44,* 1472, 1966.

Zipf, E. C., and M. R. Gorman, Electron impact excitation of the singlet states of N_2, 1, The Birge-Hopfield system ($b^1\Pi_u - X^1\Sigma_g^+$), *J. Chem. Phys., 73,* 813, 1980.

Zipf, E. C., and R. W. McLaughlin, On the dissociation of nitrogen by electron impact and by EUV photoabsorption, *Planet. Space Sci., 26,* 449, 1978.

Zipf, E. C., R.W. McLaughlin, and M. R. Gorman, Electron impact excitation of the singlet states of N_2, 2, The $c_4'\ ^1\Sigma_u^+ - X\ ^1\Sigma_g^+$ system, submitted to *J. Chem. Phys.,* 1982.

(Received June 3, 1981;
revised July 27, 1981;
accepted July 29, 1981.)